

# Numerical analysis of growth-mediated autochemotactic pattern formation in self-propelling bacteria

Jiansong Zhang<sup>a</sup>, Maosheng Jiang<sup>b</sup>, Jiang Zhu<sup>c</sup>, Xijun Yu<sup>d</sup>, Luiz Bevilacqua<sup>e</sup>

<sup>a</sup>Department of Applied Mathematics, China University of Petroleum, Qingdao 266580, China

<sup>b</sup>School of Mathematics and Statistics, Qingdao University, Qingdao 266071, China.

<sup>c</sup>Laboratório Nacional de Computação Científica, MCTI, Avenida Getúlio Vargas 333, Petrópolis, 25651-075, RJ, Brazil

<sup>d</sup>Laboratory of Computational Physics, Institute of Applied Physics and Computational Mathematics, Beijing 100088, China

<sup>e</sup>A.L. Coimbra Institute, COPPE, Federal University of Rio de Janeiro, Rio de Janeiro, Brazil

---

## Abstract

In this paper, a decoupled characteristic Galerkin finite element procedure is provided for simulating growth-mediated autochemotactic pattern formation in self-propelling bacteria. In this procedure, a modified characteristic Galerkin method is established to solve the bacterial density equation, while the classical finite element procedure is considered for the self-secreted chemical density and polarization dynamics equations system. The convergence of this proposed method is considered under some regularity assumptions and the corresponding error estimate is derived. Numerical experiments are carried out to support the theoretical analysis. Furthermore, several new wave type pattern formations are found.

**Keywords:** Self-propulsion; Wave pattern; Autochemotactic pattern formation; Error estimate; Convergence analysis.

---

## 1. Introduction

In order to investigate the spatiotemporal dynamics of a microbial colony [1, 2, 3, 4, 5], a spatially extended system of three variables with an additional term corresponding to population growth is considered: polarization  $\mathbf{p}$ , the bacterial density  $\rho$  and the self-secreted chemical density  $c$ . The reproduction and death of bacteria are modeled by considering a classic logistic growth term, which is governed by the following partial differential equations as in [1, 6, 7]:

$$\begin{cases} \text{(a)} & \frac{\partial \rho}{\partial t} = -\nabla \cdot (\rho v_0 \mathbf{p}) + D_\rho \nabla^2 \rho + \alpha \rho (1 - \rho/K), & \text{in } \Omega, \\ \text{(b)} & \frac{\partial c}{\partial t} = D_c \nabla^2 c + k_0 \rho - k_d c + k_a \nabla \cdot (\rho \mathbf{p}), & \text{in } \Omega, \\ \text{(c)} & \frac{\partial \mathbf{p}}{\partial t} = -\gamma \mathbf{p} + D_p \nabla^2 \mathbf{p} + \beta \nabla c - \gamma_2 |\mathbf{p}|^2 \mathbf{p}, & \text{in } \Omega, \end{cases}$$

where  $\Omega \subset \mathbb{R}^2$ , is a bounded rectangular domain;  $v_0$  is a constant and denotes the self-propulsion speed of the bacteria;  $D_\rho$  is the diffusion coefficient,  $\alpha$  stands for the growth rate,  $K$  is the carrying capacity of the bacteria;  $\beta$  indicates the chemotactic strength where positive  $\beta$  represents chemoattraction, while negative

---

\*Corresponding author. Maosheng Jiang

Email addresses: jszhang@upc.edu.cn (Jiansong Zhang), msjiang@qdu.edu.cn (Maosheng Jiang), jiang@lncc.br (Jiang Zhu), yuxj@iapcm.ac.cn (Xijun Yu), bevilacqua@coc.ufrj.br (Luiz Bevilacqua)

$\beta$  represents chemorepulsion.  $\gamma$  is the decay rate of  $\mathbf{p}$  and  $D_p$  is the translational diffusion constant.  $\gamma_2|\mathbf{p}|^2\mathbf{p}$  ensures the saturation of polarization at strong alignment. At a local rate  $k_0$  the chemical substance is produced from bacteria and naturally degraded at a rate  $k_d$ . The term  $k_a\nabla \cdot (\rho\mathbf{p})$  describes an anisotropic correction to the isotropic secretion term  $k_0\rho$ .

Set  $\tilde{t} = k_d t$ ,  $\tilde{\rho} = \rho/K$ , and  $\tilde{\mathbf{p}} = v_0/\sqrt{k_d D_p}\mathbf{p}$ ,  $\tilde{c} = (k_d/k_0 K)c$ . So we can rewrite the above system into an equivalent form in dimensionless quantities as follows

$$\begin{cases} \text{(a)} & \frac{\partial \rho}{\partial t} = -\nabla \cdot (\rho\mathbf{p}) + \nabla^2 \rho + g\rho(1 - \rho), & \text{in } \Omega, \\ \text{(b)} & \frac{\partial c}{\partial t} = \mathcal{D}_c \nabla^2 c + \rho - c + k\nabla \cdot (\rho\mathbf{p}), & \text{in } \Omega, \\ \text{(c)} & \frac{\partial \mathbf{p}}{\partial t} = -\Gamma\mathbf{p} + \mathcal{D}_p \nabla^2 \mathbf{p} + s\nabla c - \Gamma_2|\mathbf{p}|^2\mathbf{p}, & \text{in } \Omega, \end{cases} \quad (1.1)$$

where  $\Gamma = \gamma/k_d$ ,  $\mathcal{D}_p = D_p/D_\rho$ ,  $k = k_a k_d/(k_0 v_0)$ ,  $g = \alpha/k_d$  and  $\Gamma_2 = \gamma_2 D_p/v_0^2$ , the initial conditions are given by

$$\rho(x, 0) = \rho^0(x), \quad c(x, 0) = c^0(x), \quad \mathbf{p}(x, t) = \mathbf{p}^0(x) \quad (1.2)$$

and the periodic boundary condition is considered.

In our knowledge, there are few research works on numerical analysis of growth-mediated autochemotactic pattern formation in self-propelling bacteria. There are several interesting properties about the system, one is that many pattern formation will emerge before arriving at the steady state; the other is that, with the dynamic evolution process driven by the hydrolysis of ATP, the total free energy of the system probably increases or decreases. Therefore, many effective numerical schemes which keep energy unconditional stability, such as in [8, 9, 10, 11, 12, 13, 14, 22], could not be used. As we know, for the bacteria density equation, it is a parabolic-type equation and nonlinear convection-reaction-diffusion equation. Although there are many literature to deal with the convection-dominated [15, 16, 17, 18, 19] or reaction-diffusion problem, focusing on this model there are few work. To obtain a better approximation, we propose a new modified characteristic Galerkin finite element method for the bacterial density equation as in [20, 21, 22]. Meanwhile, the classical Galerkin finite element method could be exploited to approximate the average polarization and chemical density. As we pointed out, the new combined characteristic finite element method takes full advantages of the finite element methods and keeps the mass balance. Theoretically, we considered the convergence analysis, and derive the corresponding error estimate. Numerically, we also provide some numerical experiments to verify our theoretical results, and simulate the growth-mediated autochemotactic pattern formation in self-propelling bacteria.

We organize this paper as follows. Firstly, we will establish our new characteristic finite element method for the growth-mediated autochemotactic pattern formation in self-propelling bacteria in Section 2. Secondly, we consider the convergence of the novel method, and derive the corresponding error estimate in Section 3. And then, we find several wave pattern formation in the chemorepulsion regimes in Section 4. At last, we draw some conclusions in Section 5.

## 2. The formulation of numerical method

In this section, we will give the novel characteristic finite element method. For this purpose, we denote the characteristic direction by  $\tau$  such that

$$\phi \frac{\partial}{\partial \tau} = \frac{\partial}{\partial t} + \mathbf{p} \cdot \nabla, \quad \phi = \sqrt{1 + |\mathbf{p}|^2}.$$

So (1.1) can be rewritten into the following equivalent form

$$\begin{aligned}
\text{(a)} \quad & \phi \frac{\partial \rho}{\partial \tau} = -\nabla \cdot \mathbf{p}\rho + \nabla^2 \rho + g\rho(1 - \rho), \\
\text{(b)} \quad & \frac{\partial c}{\partial t} = \mathcal{D}_c \nabla^2 c + \rho - c + k\nabla \cdot (\rho \mathbf{p}), \\
\text{(c)} \quad & \frac{\partial \mathbf{p}}{\partial t} = \mathcal{D}_p \nabla^2 \mathbf{p} - \Gamma \mathbf{p} - \Gamma_2 |\mathbf{p}|^2 \mathbf{p} + s\nabla c.
\end{aligned} \tag{2.1}$$

To derive the time discrete scheme of system (1.1), we set  $N$  some positive integer, denote time increment  $\Delta t = T/N$ . Define a uniform time partition:  $0 =: t_0 < t_1 < \dots < t_n = n\Delta t < \dots < t_{N-1} < t_N := T$ . As in [18], we know that we can use the following formula to approximate the characteristic derivative

$$\phi \frac{\partial \rho}{\partial \tau} \approx \sqrt{1 + |\mathbf{p}^{n-1}|^2} \frac{\rho^n - \tilde{\rho}^{n-1}}{\sqrt{(X^n - x)^2 + (\Delta t)^2}} = \frac{\rho^n - \tilde{\rho}^{n-1}}{\Delta t}$$

where  $\tilde{\rho}^{n-1} = \rho(X^n)$ ,  $X^n = x - \mathbf{p}^{n-1} \Delta t$ . Hence we get the semi-discrete formulation in time of (1.1)(a) as follows

$$\frac{\rho^n - \tilde{\rho}^{n-1}}{\Delta t} + \nabla \cdot \mathbf{p}^{n-1} \rho^n - \nabla^2 \rho^n - g\rho^n(1 - \rho^{n-1}) = 0. \tag{2.2}$$

By modifying the characteristic approximation as in [20, 21],

$$\frac{\rho^n - \tilde{\rho}^{n-1} \delta^n}{\Delta t} \approx \frac{\partial \rho}{\partial t} + \nabla \cdot (\mathbf{p}\rho), \quad \delta^n = \det\left(\frac{\partial X^n}{\partial x}\right),$$

we construct a new semi-discrete formulation in time

$$\frac{\rho^n - \tilde{\rho}^{n-1} \delta^n}{\Delta t} - \nabla^2 \rho^n = g\rho^n(1 - \rho^{n-1}). \tag{2.3}$$

**Theorem 2.1** (Mass balance). *The discrete scheme (2.3) keeps mass balance.*

*Proof.* Integrating (1.1)(a) over  $t$ , we can obtain the semi-discrete mass balance equation

$$\int_{\Omega} \rho^n dx = \int_{\Omega} \rho^{n-1} dx + \int_{\Omega} g\rho^n(1 - \rho^{n-1}) dx. \tag{2.4}$$

Integrating (2.3) with respect to  $x$  on  $\Omega$ , we have

$$\int_{\Omega} \rho^n dx = \int_{\Omega} \tilde{\rho}^{n-1} \delta^n dx + \int_{\Omega} g\rho^n(1 - \rho^{n-1}) dx. \tag{2.5}$$

Using the periodic assumption and the inverse transformation, we know that

$$\int_{\Omega} \tilde{\rho}^{n-1} \delta^n dx = \int_{X^n(\Omega)} \rho^{n-1}(y) \delta^n (\delta^n)^{-1} dy = \int_{\Omega} \rho^{n-1} dx,$$

this equation suggests that (2.3) keeps mass balance.  $\square$

Based on (2.3), and time backward Euler difference scheme in time, we can get the following weak variational form

$$\begin{aligned}
\text{(a)} \quad & \left( \frac{\rho^n - \tilde{\rho}^{n-1} \delta^n}{\Delta t}, v \right) + (\nabla \rho^n, \nabla v) = (g\rho^n(1 - \rho^{n-1}), v) \quad v \in H^1(\Omega), \\
\text{(b)} \quad & \left( \frac{c^n - c^{n-1}}{\Delta t}, z \right) + (\mathcal{D}_c \nabla c^n, \nabla z) + (c^n, z) = (\rho^n + k\nabla \cdot (\rho^n \mathbf{p}^n), z) \quad z \in H^1(\Omega), \\
\text{(c)} \quad & \left( \frac{\mathbf{p}^n - \mathbf{p}^{n-1}}{\Delta t}, \mathbf{q} \right) + (\mathcal{D}_p \nabla \mathbf{p}^n, \nabla \mathbf{q}) + ([\Gamma + \Gamma_2 |\mathbf{p}^{n-1}|^2] \mathbf{p}^n, \mathbf{q}) = (s\nabla c^n, \mathbf{q}) \quad \mathbf{q} \in [H^1(\Omega)]^2.
\end{aligned} \tag{2.6}$$

Denote the uniform regular partition of the domain  $\Omega$  by  $\mathcal{T}_h$ , where the elements in the partition have the diameters bounded by  $h$ . And then, define two  $r$ -degree piecewise polynomial finite element spaces  $\mathcal{W}_h \subset [H^1(\Omega)]^2$  and  $\mathcal{V}_h \subset H^1(\Omega)$ . Based on the weak variational form (2.6), we propose the linear, decoupled characteristic Galerkin method for model problem (1.1).

### CFE Algorithm

Given initial condition  $(\rho_h^0, \mathbf{p}_h^0, c_h^0) \in \mathcal{V}_h \times \mathcal{W}_h \times \mathcal{V}_h$ , for  $n = 1, 2, \dots, N$ , seek  $(\rho_h^n, \mathbf{p}_h^n, c_h^n) \in \mathcal{V}_h \times \mathcal{W}_h \times \mathcal{V}_h$ , such that

$$\begin{aligned}
(a) \quad & \left( \frac{\rho_h^n - \tilde{\rho}_h^{n-1} \delta_h^n}{\Delta t}, v_h \right) + (\nabla \rho_h^n, \nabla v_h) = (g \rho_h^n (1 - \rho_h^{n-1}), v_h) \quad \forall v_h \in \mathcal{V}_h, \\
(b) \quad & \left( \frac{c_h^n - c_h^{n-1}}{\Delta t}, z_h \right) + (\mathcal{D}_c \nabla c_h^n, \nabla z_h) + (c_h^n, z_h) = (\rho_h^n + k \nabla \cdot (\rho_h^n \mathbf{p}_h^{n-1}), z_h) \quad \forall z_h \in \mathcal{V}_h, \\
(c) \quad & \left( \frac{\mathbf{p}_h^n - \mathbf{p}_h^{n-1}}{\Delta t}, \mathbf{q}_h \right) + (\mathcal{D}_p \nabla \mathbf{p}_h^n, \nabla \mathbf{q}_h) + ([\Gamma + \Gamma_2 |\mathbf{p}_h^{n-1}|^2] \mathbf{p}_h^n, \mathbf{q}_h) = (s \nabla c_h^n, \mathbf{q}_h) \quad \mathbf{q}_h \in \mathcal{W}_h,
\end{aligned} \tag{2.7}$$

where  $\tilde{\rho}_h^{n-1} = \rho(X_h^n)$ ,  $X_h^n = x - \mathbf{p}_h^{n-1} \Delta t$ ,  $\delta_h^n = \det(\partial X_h^n / \partial x)$ .

For CFE Algorithm, we can get the main convergence theorem as follows:

**Theorem 2.2.** *Let  $(\rho_h^n, \mathbf{p}_h^n, c_h^n)$  be the solution of CFE Algorithm. If the regularities of the solution  $(\rho^n, \mathbf{p}^n, c^n)$  of the model problem (1.1):  $\rho \in l^\infty(W^{1,\infty})$ ,  $\rho_t \in l^2(H^{r+1})$ ,  $\rho_{tt} \in l^2(L^2)$ ,  $\mathbf{p} \in l^\infty(W^{1,\infty})$ ,  $\mathbf{p}_t \in l^2(H^{r+1})$ ,  $\mathbf{p}_{tt} \in l^2(L^2)$ ,  $c \in l^\infty(W^{1,\infty})$ ,  $c_t \in l^2(H^{r+1})$ ,  $c_{tt} \in l^2(L^2)$  hold, the following error estimate holds*

$$\max_n \|\rho^n - \rho_h^n\|_{L^2} + \max_n \|\mathbf{p}^n - \mathbf{p}_h^n\|_{L^2} + \max_n \|\sigma^n - \sigma_h^n\|_{L^2} \leq C\{h^{r+1} + \Delta t\}. \tag{2.8}$$

### 3. Convergence analysis

In order to prove our convergence theorem, as in [23], we introduce two elliptic projection operators  $\Pi_h$  and  $\Pi_p$  such that

$$(\nabla w, \nabla v_h) = (\nabla \Pi_h w, \nabla v_h), \quad \forall v_h \in \mathcal{V}_h, \quad (\nabla \mathbf{p}, \nabla \mathbf{q}_h) = (\nabla \Pi_p \mathbf{p}, \nabla \mathbf{q}_h), \quad \forall \mathbf{q}_h \in \mathcal{W}_h. \tag{3.1}$$

The following approximate properties hold

$$\begin{aligned}
(a) \quad & \|w - \Pi_h w\|_{L^2} + h \|\nabla(w - \Pi_h w)\|_{[L^2]^2} \leq Ch^{r+1} \|w\|_{H^{r+1}}, \quad \forall w \in H^{r+1}(\Omega), \\
(b) \quad & \|\mathbf{p} - \Pi_p \mathbf{p}\|_{[L^2]^2} + h \|\nabla(\mathbf{p} - \Pi_p \mathbf{p})\|_{[L^2]^2} \leq Ch^{r+1} \|\mathbf{p}\|_{[H^{r+1}]^2}, \quad \forall \mathbf{p} \in [H^{r+1}(\Omega)]^2.
\end{aligned} \tag{3.2}$$

And the estimates can be easily obtained as follows:

$$\begin{aligned}
(a) \quad & \|(w - \Pi_h w)_t\|_{L^2} \leq Ch^{r+1} \|w_t\|_{H^{r+1}}, \quad \forall w \in H^{r+1}(\Omega), \\
(b) \quad & \|(\mathbf{p} - \Pi_p \mathbf{p})_t\|_{[L^2]^2} \leq Ch^{r+1} \|\mathbf{p}_t\|_{[H^{r+1}]^2}, \quad \forall \mathbf{p} \in [H^{r+1}(\Omega)]^2.
\end{aligned} \tag{3.3}$$

Set

$$\begin{aligned}
\rho_h^n - \rho^n &= (\rho_h^n - \Pi_h \rho^n) - (\rho^n - \Pi_h \rho^n) = \theta_\rho^n - \zeta_\rho^n, \\
\mathbf{p}_h^n - \mathbf{p}^n &= (\mathbf{p}_h^n - \Pi_p \mathbf{p}^n) - (\mathbf{p}^n - \Pi_p \mathbf{p}^n) = \theta_p^n - \zeta_p^n, \\
c_h^n - c^n &= (c_h^n - \Pi_h c^n) - (c^n - \Pi_h c^n) = \theta_c^n - \zeta_c^n.
\end{aligned}$$

Subtracting (2.1) from (2.7), we can get the following error residual equations

$$\begin{aligned}
& \left( \frac{\theta_\rho^n - \tilde{\theta}_\rho^{n-1} \delta_h^n}{\Delta t}, v_h \right) + (\nabla \theta_\rho^n, \nabla v_h) \\
&= \left( \frac{\zeta_\rho^n - \tilde{\zeta}_\rho^{n-1} \delta_h^n}{\Delta t}, v_h \right) + \left( \frac{\tilde{\rho}_h^{n-1} (\delta_h^n - \delta^n)}{\Delta t}, v_h \right) + (g \rho_h^n (1 - \rho_h^{n-1}) - g \rho^n (1 - \rho^n), v_h) \\
& \quad + \left( \frac{(\tilde{\rho}_h^{n-1} - \tilde{\rho}^{n-1}) \delta^n}{\Delta t}, v_h \right) + \left( \frac{\partial \rho^n}{\partial t} - \frac{\rho^n - \tilde{\rho}^{n-1} \delta^n}{\Delta t}, v_h \right),
\end{aligned} \tag{3.4}$$

$$\begin{aligned}
\left( \frac{\theta_c^n - \theta_c^{n-1}}{\Delta t}, z_h \right) + (\mathcal{D}_c \nabla \theta_c^n, \nabla z_h) + (\theta_c^n, z_h) &= \left( \frac{\zeta_c^n - \zeta_c^{n-1}}{\Delta t}, z_h \right) + \left( \frac{\partial c^n}{\partial t} - \frac{c^n - c^{n-1}}{\Delta t}, z_h \right) + (\zeta_c^n, z_h) \\
& \quad + (\rho_h^n - \rho^n, z_h) + (k \nabla \cdot (\rho_h^n \mathbf{p}_h^{n-1} - \rho^n \mathbf{p}^n), z_h),
\end{aligned} \tag{3.5}$$

and

$$\begin{aligned}
\left( \frac{\theta_p^n - \theta_p^{n-1}}{\Delta t}, \mathbf{q}_h \right) + (\mathcal{D}_p \nabla \theta_p^n, \nabla \mathbf{q}_h) &= \left( \frac{\zeta_p^n - \zeta_p^{n-1}}{\Delta t}, \mathbf{q}_h \right) + \left( \frac{\partial \mathbf{p}^n}{\partial t} - \frac{\mathbf{p}^n - \mathbf{p}^{n-1}}{\Delta t}, \mathbf{q}_h \right) - (\Gamma[\mathbf{p}_h^n - \mathbf{p}^n], \mathbf{q}_h) \\
& \quad - (\Gamma_2[|\mathbf{p}_h^{n-1}|^2 \mathbf{p}_h^n - |\mathbf{p}^n|^2 \mathbf{p}^n], \mathbf{q}_h) + (s \nabla (c_h^n - c^n), \mathbf{q}_h).
\end{aligned} \tag{3.6}$$

For the proof of Theorem 2.2, the inductive hypothesis is necessary

$$\max_n \|\mathbf{p}_h^n\|_{L^\infty} + \max_n \|\rho_h^n\|_{L^\infty} \leq C < +\infty. \tag{3.7}$$

Now we estimate the boundedness of  $\theta_\rho^n$ ,  $\theta_p^n$  and  $\theta_c^n$  one by one when the hypothesis (3.7) holds until  $k = n - 1$ .

### 3.1. The estimate of $\theta_p^n$

**Lemma 3.1.** For  $\theta_p^n$ , we have the estimate

$$\|\theta_p^n\|_{L^2}^2 + \Delta t \sum_{i=1}^n \|\nabla \theta_p^i\|_{L^2}^2 \leq C \{ \Delta t \sum_{i=1}^n [\|\theta_p^i\|_{L^2}^2 + \|\theta_c^i\|_{L^2}^2] + h^{2r+2} + \Delta t^2 \}. \tag{3.8}$$

*Proof.* Choosing  $\mathbf{q}_h = \theta_p^n$  in (3.6) we have

$$\begin{aligned}
& \frac{1}{2\Delta t} [(\theta_p^n, \theta_p^n) - (\theta_p^{n-1}, \theta_p^{n-1})] + (\mathcal{D}_p \nabla \theta_p^n, \nabla \theta_p^n) \\
& \leq \left( \frac{1}{\Delta t} \int_{t_{n-1}}^{t_n} \frac{\partial \zeta_p}{\partial t} dt, \theta_p^n \right) + \left( \frac{\partial \mathbf{p}^n}{\partial t} - \frac{\mathbf{p}^n - \mathbf{p}^{n-1}}{\Delta t}, \theta_p^n \right) \\
& \quad - (\Gamma[\mathbf{p}_h^n - \mathbf{p}^n] + \Gamma_2[|\mathbf{p}_h^{n-1}|^2 \mathbf{p}_h^n - |\mathbf{p}^n|^2 \mathbf{p}^n], \theta_p^n) \\
& \quad + (s \nabla (c_h^n - c^n), \theta_p^n) = E_1 + E_2 + E_3 + E_4.
\end{aligned} \tag{3.9}$$

Note that

$$E_1 + E_2 \leq C \left\{ \frac{1}{\Delta t} \int_{t_{n-1}}^{t_n} \left\| \frac{\partial \zeta_p}{\partial t} \right\|_{L^2}^2 dt + \Delta t \int_{t_{n-1}}^{t_n} \|\mathbf{p}_h^n\|_{L^2}^2 dt + \|\theta_p^n\|_{L^2}^2 \right\}$$

and

$$E_4 = -(s(c_h^n - c^n), \nabla \cdot \theta_p^n) \leq C \{ \|\theta_c^n\|_{L^2}^2 + \|\zeta_c^n\|_{L^2}^2 \} + \frac{1}{2} \|\mathcal{D}_p^{1/2} \nabla \theta_p^n\|_{L^2}^2.$$

Then, we can give the estimate of  $E_3$ . We know that

$$\begin{aligned}
E_3 &= -(\Gamma[\mathbf{p}_h^n - \mathbf{p}^n], \theta_p^n) - (\Gamma_2[|\mathbf{p}_h^{n-1}|^2 \mathbf{p}_h^n - |\mathbf{p}^n|^2 \mathbf{p}^n], \theta_p^n) \\
&= -(\Gamma[\mathbf{p}_h^n - \mathbf{p}^n], \theta_p^n) - (\Gamma_2|\mathbf{p}_h^{n-1}|^2(\mathbf{p}_h^n - \mathbf{p}^n), \theta_p^n) \\
&\quad - (\Gamma_2(\mathbf{p}_h^{n-1} + \mathbf{p}^n) \cdot \mathbf{p}^n(\mathbf{p}_h^{n-1} - \mathbf{p}^n), \theta_p^n) \\
&\leq C\{\|\theta_p^n\|_{L^2}^2 + \|\zeta_p^n\|_{L^2}^2 + \|\theta_p^{n-1}\|_{L^2}^2 + \|\zeta_p^n\|_{L^2}^2 + \Delta t \int_{t_{n-1}}^{t_n} \|\mathbf{p}_t\|_{L^2}^2 dt\},
\end{aligned}$$

where the inductive hypothesis (3.7) has been used in the last inequality.

Substituting these estimates into (3.9), we get the estimate

$$\begin{aligned}
&\frac{1}{2\Delta t} [(\theta_p^n, \theta_p^n) - (\theta_p^{n-1}, \theta_p^{n-1})] + \frac{1}{2} (\mathcal{D}_p \nabla \theta_p^n, \nabla \theta_p^n) \\
&\leq C\{\|\theta_p^n\|_{L^2}^2 + \|\theta_p^{n-1}\|_{L^2}^2 + \|\theta_c^n\|_{L^2}^2 + \|\zeta_p^n\|_{L^2}^2 + \|\zeta_c^n\|_{L^2}^2 \\
&\quad + \frac{1}{\Delta t} \int_{t_{n-1}}^{t_n} \|\frac{\partial \zeta_p}{\partial t}\|_{L^2}^2 dt + \Delta t \int_{t_{n-1}}^{t_n} (\|\mathbf{p}_t\|_{L^2}^2 + \|\mathbf{p}_{tt}\|_{L^2}^2) dt\}.
\end{aligned}$$

Multiplying it by  $2\Delta t$ , and summing it over  $n$ , then we can obtain

$$\begin{aligned}
\|\theta_p^n\|_{L^2}^2 + \Delta t \sum_{i=1}^n \|\nabla \theta_p^i\|_{L^2}^2 &\leq C\{\Delta t \sum_{i=1}^n [\|\theta_p^i\|_{L^2}^2 + \|\zeta_p^i\|_{L^2}^2 + \|\theta_c^i\|_{L^2}^2 + \|\zeta_c^i\|_{L^2}^2] \\
&\quad + \|\frac{\partial \zeta_p}{\partial t}\|_{L^2(0,t_n;L^2)}^2 + \Delta t^2 (\|\mathbf{p}_t\|_{L^2(0,t_n;L^2)}^2 + \|\mathbf{p}_{tt}\|_{L^2(0,t_n;L^2)}^2)\}.
\end{aligned} \tag{3.10}$$

By use of the estimate (3.2), we know that the estimate (3.8) holds.  $\square$

### 3.2. The estimate of $\theta_p^n$

**Lemma 3.2.** For  $\theta_p^n$ , we have the estimate

$$\|\theta_p^n\|_{L^2}^2 + \Delta t \sum_{i=1}^n \|\nabla \theta_p^i\|_{L^2}^2 \leq C\{\Delta t \sum_{i=1}^n [\|\theta_p^{i-1}\|_{L^2}^2 + \|\theta_p^{i-1}\|_{L^2}^2] + h^{2r+2} + \Delta t^2\}. \tag{3.11}$$

*Proof.* Taking  $v_h = \theta_p^n$  in (3.4), we can get then we can get

$$\begin{aligned}
&(\frac{\theta_p^n - \tilde{\theta}_p^{n-1} \delta_h^n}{\Delta t}, \theta_p^n) + (\nabla \theta_p^n, \nabla \theta_p^n) \\
&= (\frac{\partial \rho^n}{\partial t} - \frac{\rho^n - \tilde{\rho}^{n-1} \delta_h^n}{\Delta t}, \theta_p^n) + (\frac{(\tilde{\rho}_h^{n-1} - \tilde{\rho}^{n-1}) \delta_h^n}{\Delta t}, \theta_p^n) + (\frac{\tilde{\rho}_h^{n-1} (\delta_h^n - \delta^n)}{\Delta t}, \theta_p^n) \\
&\quad + (\frac{\zeta_p^n - \tilde{\zeta}_p^{n-1} \delta_h^n}{\Delta t}, \theta_p^n) + (g(1 + \rho_h^{n-1})(\theta_p^n - \zeta_p^n), \theta_p^n) \\
&\quad + (g\rho^n(\theta_p^{n-1} - \zeta_p^{n-1}), \theta_p^n) - (g\rho^n \int_{t_{n-1}}^{t_n} \rho_t dt, \theta_p^n) = T_1 + T_2 + T_3 + \dots + T_7.
\end{aligned} \tag{3.12}$$

Using the same technique as in [20], we can get the inequality

$$|T_1 + T_2| \leq C\{\Delta t^2 \|\rho\|_{C^2(L^2) \cap C^1(H^1) \cap C^2(H^2)}^2 + \|\mathbf{p}_h^{n-1} - \mathbf{p}^{n-1}\|_{L^2}^2\} + \frac{\varepsilon}{4} \|\theta_p^n\|_{L^2}^2.$$

Utilizing the definition of  $\delta^n$  and  $\delta_h^n$ , we know that

$$\delta^n = 1 - \Delta t \nabla \cdot \mathbf{p}^{n-1} + O(\Delta t^2), \quad \delta_h^n = 1 - \Delta t \nabla \cdot \mathbf{p}_h^{n-1} + O(\Delta t^2).$$

So for  $T_3$  we have

$$|T_3| \leq C \|\mathbf{p}_h^{n-1} - \mathbf{p}^{n-1}\|_{L^2}^2 + \frac{\varepsilon}{4} \|\nabla \theta_\rho^n\|_{L^2}^2.$$

For  $T_4$ , we have

$$\begin{aligned} T_4 &= \left( \frac{\zeta_\rho^n - \zeta_\rho^{n-1}}{\Delta t}, \theta_\rho^n \right) + \left( \frac{\zeta_\rho^{n-1} - \tilde{\zeta}_\rho^{n-1} \delta_h^n}{\Delta t}, \theta_\rho^n \right) \\ &= \left( \frac{\zeta_\rho^n - \zeta_\rho^{n-1}}{\Delta t}, \theta_\rho^n \right) + \left( \frac{\tilde{\zeta}_\rho^{n-1} \delta_h^n}{\Delta t}, \tilde{\theta}^n \right) - \left( \frac{\tilde{\zeta}_\rho^{n-1} \delta_h^n}{\Delta t}, \theta_\rho^n \right) \\ &= \left( \frac{\zeta_\rho^n - \zeta_\rho^{n-1}}{\Delta t}, \theta_\rho^n \right) + \left( \tilde{\zeta}_\rho^{n-1} \delta_h^n, \frac{\tilde{\theta}^n - \theta_\rho^n}{\Delta t} \right). \end{aligned} \tag{3.13}$$

To estimate the bound of  $T_4$ , we consider the following transformation,

$$y = f_{\bar{z}} = x - \mathbf{p}_h^{n-1} \Delta t \bar{z}.$$

It is easily seen that

$$\begin{aligned} \left\| \frac{\tilde{\theta}^n - \theta_\rho^n}{\Delta t} (\delta_h^n)^{1/2} \right\|_{L^2}^2 &= \Delta t^{-2} \int_{\Omega} (\theta_\rho^n - \tilde{\theta}^n)^2 \delta_h^n dx = \Delta t^{-2} \int_{\Omega} \left( \int_{x_h^n}^x \frac{\partial \theta_\rho^n}{\partial z} dz \right)^2 \delta_h^n dx \\ &= \Delta t^{-2} \int_{\Omega} \left( \int_0^1 \frac{\partial \theta_\rho^n}{\partial z} (x - \mathbf{p}_h^{n-1} \Delta t \bar{z}) \cdot (\mathbf{p}_h^{n-1} \Delta t \bar{z}) d\bar{z} \right)^2 \delta_h^n dx \\ &\leq C \int_0^1 \int_{\Omega} |\nabla \theta_\rho^n (x - \mathbf{p}_h^{n-1} \Delta t \bar{z})|^2 \delta_h^n dx d\bar{z} \leq C \|\nabla \theta_\rho^n\|_{L^2}^2. \end{aligned}$$

Using the above inequality, we can get

$$\begin{aligned} |T_4| &\leq \left\| \frac{\zeta_\rho^n - \zeta_\rho^{n-1}}{\Delta t} \right\|_{L^2} \|\theta_\rho^n\|_{L^2} + \|\tilde{\zeta}_\rho^{n-1} (\delta_h^n)^{1/2}\|_{L^2} \left\| \frac{\tilde{\theta}^n - \theta_\rho^n}{\Delta t} (\delta_h^n)^{1/2} \right\|_{L^2} \\ &\leq C \left\{ \frac{1}{\Delta t} \int_{t_{n-1}}^{t_n} \left\| \frac{\zeta_\rho}{\partial t} \right\|_{L^2}^2 dt + \|\zeta_\rho^{n-1}\|_{L^2}^2 \right\} + \frac{\varepsilon}{4} \|\nabla \theta_\rho^n\|_{L^2}^2. \end{aligned}$$

For  $T_5$ ,  $T_6$  and  $T_7$ , using Schwarz inequality, we can get

$$T_5 + T_6 + T_7 \leq C \{ \|\theta_\rho^n\|_{L^2}^2 + \|\theta_\rho^{n-1}\|_{L^2}^2 + \|\zeta_\rho^n\|_{L^2}^2 + \|\zeta_\rho^{n-1}\|_{L^2}^2 + \Delta t \int_{t_{n-1}}^{t_n} \|\rho_t\|_{L^2}^2 dt \}$$

Substituting the above estimates into (3.12), we get

$$\begin{aligned} &\left( \frac{\theta_\rho^n - \tilde{\theta}^{n-1} \delta_h^n}{\Delta t}, \theta_\rho^n \right) + (\nabla \theta_\rho^n, \nabla \theta_\rho^n) \\ &\leq C \{ \|\theta_\rho^n\|_{L^2}^2 + \|\theta_\rho^{n-1}\|_{L^2}^2 + \|\theta_\rho^{n-1}\|_{L^2}^2 + \|\zeta_\rho^{n-1}\|_{L^2}^2 + \|\zeta_\rho^n\|_{L^2}^2 + \|\zeta_\rho^{n-1}\|_{L^2}^2 \\ &\quad + \Delta t \int_{t_{n-1}}^{t_n} \|\rho_t\|_{L^2}^2 dt + \frac{1}{\Delta t} \int_{t_{n-1}}^{t_n} \left\| \frac{\partial \zeta_\rho}{\partial t} \right\|_{L^2}^2 dt \\ &\quad + \Delta t^2 \|\rho\|_{C^2(L^2) \cap C^1(H^1) \cap C^2(H^2)}^2 \} + \frac{\varepsilon}{2} [ \|\theta_\rho^n\|_{L^2}^2 + \|\nabla \theta_\rho^n\|_{L^2}^2 ]. \end{aligned}$$

It is easily seen that

$$\begin{aligned} \left( \frac{\theta_\rho^n - \tilde{\theta}_\rho^{n-1} \delta_h^n}{\Delta t}, \theta_\rho^n \right) &\geq \frac{1}{2\Delta t} [\|\theta_\rho^n\|_{L^2}^2 - \|\tilde{\theta}_\rho^{n-1} \delta_h^n\|_{L^2}^2] \\ &\geq \frac{1}{2\Delta t} [\|\theta_\rho^n\|_{L^2}^2 - (1 + C\Delta t)\|\theta_\rho^{n-1}\|_{L^2}^2]. \end{aligned}$$

Hence, for sufficiently small  $\varepsilon$ , we have

$$\begin{aligned} &\|\theta_\rho^n\|_{L^2}^2 - \|\theta_\rho^{n-1}\|_{L^2}^2 + \Delta t \|\nabla \theta_\rho^n\|_{L^2}^2 \\ &\leq C\Delta t \{ \|\theta_\rho^n\|_{L^2}^2 + \|\theta_\rho^{n-1}\|_{L^2}^2 + \|\theta_\rho^{n-1}\|_{L^2}^2 + \|\zeta_p^{n-1}\|_{L^2}^2 + \|\zeta_\rho^n\|_{L^2}^2 + \|\zeta_\rho^{n-1}\|_{L^2}^2 + \Delta t \int_{t_{n-1}}^{t_n} \|\rho_t\|_{L^2}^2 dt \\ &\quad + \frac{1}{\Delta t} \int_{t_{n-1}}^{t_n} \left\| \frac{\partial \zeta_\rho}{\partial t} \right\|_{L^2}^2 dt + \Delta t^2 \|\rho\|_{C^2(L^2) \cap C^1(H^1) \cap C^2(H^2)}^2 \}. \end{aligned}$$

Summing the estimate from 1 to  $n$ , we get

$$\begin{aligned} &\|\theta_\rho^n\|_{L^2}^2 + \Delta t \sum_{i=1}^n \|\nabla \theta_\rho^i\|_{L^2}^2 \\ &\leq C\Delta t \sum_{i=1}^n [\|\theta_\rho^i\|_{L^2}^2 + \|\zeta_\rho^i\|_{L^2}^2 + \|\theta_\rho^{i-1}\|_{L^2}^2 + \|\zeta_\rho^{i-1}\|_{L^2}^2] + \left\| \frac{\partial \zeta_\rho}{\partial t} \right\|_{L^2(0,t_n;L^2)}^2 \\ &\quad + \Delta t^2 \|\rho_t\|_{L^2(0,t_n;L^2)}^2 + \Delta t^2 \|\rho\|_{C^2(L^2) \cap C^1(H^1) \cap C^2(H^2)}^2 \}. \end{aligned} \tag{3.14}$$

Using the estimates (3.2) and (3.3), we get the inequality (3.11).  $\square$

### 3.3. The estimate of $\theta_c^n$

**Lemma 3.3.** For  $\theta_c^n$ , we have the estimate

$$\|\theta_c^n\|_{L^2}^2 + \Delta t \sum_{i=1}^n \|\nabla \theta_c^i\|_{L^2}^2 \leq C\{\Delta t \sum_{i=1}^n [\|\theta_c^{i-1}\|_{L^2}^2 + \|\theta_c^i\|_{L^2}^2] + h^{2r+2} + \Delta t^2\}. \tag{3.15}$$

*Proof.* Choosing  $z_h = \theta_c^n$  in (3.5), we can get

$$\begin{aligned} &\frac{1}{2\Delta t} [\|\theta_c^n\|_{L^2}^2 - \|\theta_c^{n-1}\|_{L^2}^2] + (\mathcal{D}_c \nabla \theta_c^n, \nabla \theta_c^n) + \|\theta_c^n\|_{L^2}^2 \\ &\leq \left( \frac{\zeta_c^n - \zeta_c^{n-1}}{\Delta t}, \theta_c^n \right) + \left( \frac{\partial c^n}{\partial t} - \frac{c^n - c^{n-1}}{\Delta t}, \theta_c^n \right) + (\zeta_c^n, \theta_c^n) \\ &\quad + (\rho_h^n - \rho^n, \theta_c^n) + (k \nabla \cdot (\rho_h^n \mathbf{p}_h^{n-1} - \rho^n \mathbf{p}^n), \theta_c^n) \\ &= I_1 + I_2 + \dots + I_5. \end{aligned} \tag{3.16}$$

For  $I_1, I_2, I_3$  and  $I_4$ , we have the estimate

$$I_1 + I_2 + I_3 + I_4 \leq C \left\{ \int_{t_{n-1}}^{t_n} \left\| \frac{\partial \zeta_c}{\partial t} \right\|_{L^2}^2 dt + \Delta t \int_{t_{n-1}}^{t_n} \|c_{tt}\|_{L^2}^2 dt + \|\zeta_c^n\|_{L^2}^2 + \|\theta_c^n\|_{L^2}^2 + \|\zeta_\rho^n\|_{L^2}^2 \right\} + \frac{1}{2} \|\theta_c^n\|_{L^2}^2.$$

Note that

$$\begin{aligned} I_5 &= - (k[(\rho_h^n - \rho^n) \mathbf{p}_h^{n-1}], \nabla \theta_c^n) - (k[\rho^n (\mathbf{p}_h^{n-1} - \mathbf{p}^{n-1})], \nabla \theta_c^n) - (k[\rho^n (\mathbf{p}^{n-1} - \mathbf{p}^n)], \nabla \theta_c^n) \\ &\leq C \{ \|\theta_\rho^n\|_{L^2}^2 + \|\theta_\rho^{n-1}\|_{L^2}^2 + \|\zeta_\rho^n\|_{L^2}^2 + \|\zeta_\rho^{n-1}\|_{L^2}^2 + \Delta t \int_{t_{n-1}}^{t_n} \|\mathbf{p}_t\|_{L^2}^2 dt \} + \frac{1}{2} \Delta t \|\mathcal{D}_c^{1/2} \nabla \theta_c^n\|_{L^2}^2. \end{aligned}$$



Substituting the above estimates into (3.16) and multiplying it by  $2\Delta t$ , we get

$$\begin{aligned} & \|\theta_c^n\|_{L^2}^2 - \|\theta_c^{n-1}\|_{L^2}^2 + \Delta t \|\mathcal{D}_c^{1/2} \nabla \theta_c^n\|_{L^2}^2 \\ & \leq C \Delta t \left\{ \frac{1}{\Delta t} \int_{t_{n-1}}^{t_n} \left\| \frac{\partial \zeta_c}{\partial t} \right\|_{L^2}^2 dt + \|\zeta_c^n\|_{L^2}^2 + \|\zeta_p^n\|_{L^2}^2 + \|\zeta_p^{n-1}\|_{L^2}^2 + \|\theta_p^n\|_{L^2}^2 \right. \\ & \quad \left. + \|\theta_p^{n-1}\|_{L^2}^2 + \Delta t \int_{t_{n-1}}^{t_n} [\|\mathbf{p}_t\|_{L^2}^2 + \|c_{tt}\|_{L^2}^2] dt \right\}. \end{aligned}$$

Hence, utilizing (3.2) and summing the above estimate from 1 to  $n$ , we can obtain the inequality (3.15).  $\square$

### 3.4. The proof of Theorem 2.2

*Proof.* Utilizing Lemmas 3.1-3.3, we have the estimate

$$\begin{aligned} & \|\theta_p^n\|_{L^2}^2 + \|\theta_p^{n-1}\|_{L^2}^2 + \|\theta_c^n\|_{L^2}^2 + \Delta t \sum_{i=1}^n [\|\nabla \theta_p^i\|_{L^2}^2 + \|\nabla \theta_p^{i-1}\|_{L^2}^2 + \|\nabla \theta_c^i\|_{L^2}^2] \\ & \leq C \left\{ \Delta t \sum_{i=1}^n [\|\theta_p^{i-1}\|_{L^2}^2 + \|\theta_c^{i-1}\|_{L^2}^2 + \|\theta_p^{i-1}\|_{L^2}^2] + h^{2r+2} + \Delta t^2 \right\}. \end{aligned} \quad (3.17)$$

The discrete Gronwall's lemma results in the estimate

$$\|\theta_p^n\|_{L^2}^2 + \|\theta_p^{n-1}\|_{L^2}^2 + \|\theta_c^n\|_{L^2}^2 + \Delta t \sum_{i=1}^n [\|\nabla \theta_p^i\|_{L^2}^2 + \|\nabla \theta_p^{i-1}\|_{L^2}^2 + \|\nabla \cdot \theta_c^i\|_{L^2}^2] \leq C \{h^{2r+2} + \Delta t^2\} \quad (3.18)$$

Utilizing the approximate properties (3.2), we the convergence result of Theorem 2.2.

Finally we check the inductive hypothesis (3.7). From (3.18), we can get the estimate

$$\begin{aligned} \|\mathbf{p}_h^n\|_{L^\infty} + \|\rho_h^n\|_{L^\infty} & \leq Ch^{-1} \{ \|\theta_p^n\|_{L^2} + \|\theta_p^{n-1}\|_{L^2} \} + (\|\zeta_p^n\|_{L^\infty} + \|\zeta_p^{n-1}\|_{L^\infty} + \|p^n\|_{L^\infty} + \|p^{n-1}\|_{L^\infty}) \\ & \leq Ch^{-1} (h^{r+1} + \Delta t) + Ch^{r+1} + \|\mathbf{p}^n\|_{L^\infty} + \|p^n\|_{L^\infty} \leq C, \end{aligned} \quad (3.19)$$

So, the inductive hypothesis (3.7) holds.  $\square$

## 4. Numerical examples

### 4.1. Convergence test

Set  $\Omega = [0, 1] \times [0, 1]$ . We show several numerical results for the coupled problem (1.1) with our proposed method. The coefficients of the coupled system (1.1) can be chosen as follows:

$$D_c = 1, \quad D_p = 1, \quad s = 0.5, \quad k = 1, \quad \Gamma = 1, \quad \Gamma_2 = 10, \quad g = 0.1.$$

The exact solution of the coupled system (1.1) is taken by

$$\begin{aligned} \rho(x, y, t) &= \sin(4\pi x) \sin(4\pi y) \exp(\sin(t)) \\ c(x, y, t) &= \cos(4\pi x) \cos(4\pi y) \exp(\cos(t)), \\ p_1(x, y, t) &= \sin(4\pi x) \cos(4\pi y) \exp(\sin(t)), \\ p_2(x, y, t) &= \cos(4\pi x) \sin(4\pi y) \exp(\cos(t)). \end{aligned} \quad (4.20)$$

The piecewise linear polynomial space is considered. For different mesh size  $h$  and  $\Delta t = h^2$ , some numerical results are presented in Table 1, Table 2 and Table 3 for  $\rho$ ,  $c$  and  $\|\mathbf{P}\|$ , where  $\|\mathbf{P}\|^2 = \int_{\Omega} (p_1^2 +$

$p_2^2)dx$ . From these tables, we can easily see that the new method is of time first-order accuracy and spacial second-order accuracy both in  $L^2$ -norm and  $L^\infty$ -norm, which is coincided with theoretical result.

Table 1: Convergence results for  $\rho$

$h$	Convergence rates in space				Convergence rates in time			
	$L^\infty$	rate	$L^2$	rate	$L^\infty$	rate	$L^2$	rate
1/8	9.61e-02	-	7.68e-02	-	9.61e-02	-	7.68e-02	-
1/16	2.41e-02	2.0	1.01e-02	2.0	2.41e-02	1.0	1.01e-02	1.0
1/32	6.02e-03	2.0	2.25e-03	2.0	6.02e-03	1.0	2.25e-03	1.0
1/64	1.52e-03	2.0	5.61e-04	2.0	1.52e-03	1.0	5.61e-04	1.0

Table 2: Convergence results for  $c$

$h$	Convergence rates in space				Convergence rates in time			
	$L^\infty$	rate	$L^2$	rate	$L^\infty$	rate	$L^2$	rate
1/8	2.13e-01	-	1.52e-01	-	2.13e-01	-	1.52e-01	-
1/16	5.22e-02	2.0	3.79e-02	2.0	5.22e-02	1.0	3.79e-02	1.0
1/32	1.28e-02	2.0	9.45e-03	2.0	1.28e-02	1.0	9.45e-03	1.0
1/64	3.01e-03	2.0	2.35e-03	2.0	3.01e-03	1.0	2.35e-03	1.0

Table 3: Convergence results for  $\|\mathbf{P}\|$

$h$	Convergence rates in space				Convergence rates in time			
	$L^\infty$	rate	$L^2$	rate	$L^\infty$	rate	$L^2$	rate
1/8	1.70e-01	-	1.28e-01	-	1.70e-01	-	1.28e-01	-
1/16	4.20e-02	2.0	3.18e-02	2.0	4.20e-02	1.0	3.18e-02	1.0
1/32	1.03e-02	2.0	7.93e-03	2.0	1.03e-02	1.0	7.93e-03	1.0
1/64	2.55e-03	2.0	1.95e-03	2.0	2.55e-03	1.0	1.95e-03	1.0

In order to validate the efficiency of our proposed method in the following subsections, we will give some numerical results to simulate dynamics of the clustering and pattern formation in the repulsion case as listed in [6? ], meanwhile, we will consider some other value of parameter to try find the new wave pattern formation. Throughout the following section, the parameters are chosen as follows:

$$D_c = 1.0, \Gamma_2 = 10, \Gamma = 1.0, D_p = 1.0, k = 0.5.$$

The mesh size and time increment are 0.34 and 0.01, respectively. The period boundary condition is still considered.

#### 4.2. Chemorepulsion case 1

In this case, the initial profile of bacterial density, self-chemical density and polarization given as  $(u_0, c_0, \mathbf{p}_0)$ .  $u_0 = 0.1 \exp(-200*(x-0.5*Lx)^2 - 200*(y-0.5*Ly)^2)$ ,  $c_0 = u_0$ ,  $\mathbf{p}_0 = 0.01(\text{rand}(0, 1), \text{rand}(0, 1))$ ,  $Lx = 60$ ,  $Ly = 60$ ,  $d = 0.01$ ,  $h = 0.6$ . The evolution of the process is shown as in Fig.1-3. These numerical results show that clustering and pattern formation appear with the increase of time, and finally both of them form one special order. It seems that firstly the regular clustering appears and parallel to the

boundary of domain as shown in Fig.2e and Fig.1f, secondly, the total clustering gathering into four parts as represented in Fig.2f and Fig.1h, thirdly, each part following the counter-diagonal direction move as Fig.2g, finally all the parts move in the same velocity and small clustering is back to one whole as Fig.2h. Then the pattern will get into the first step. The process of this cycle never stops. The system arrives at one equilibrium state. The Fig.3 shows the dynamic process of polarization which clearly represent pattern formation and wave appears association with bacteria and self-secreted chemical.

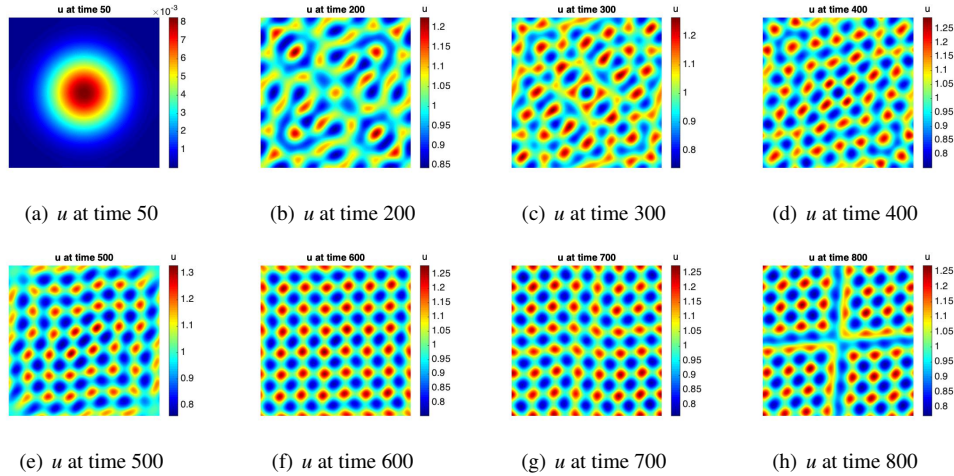


Figure 1: The dynamic process for bacterial density with small initial distribution and  $s = -15$ ,  $g = 0.1$ .

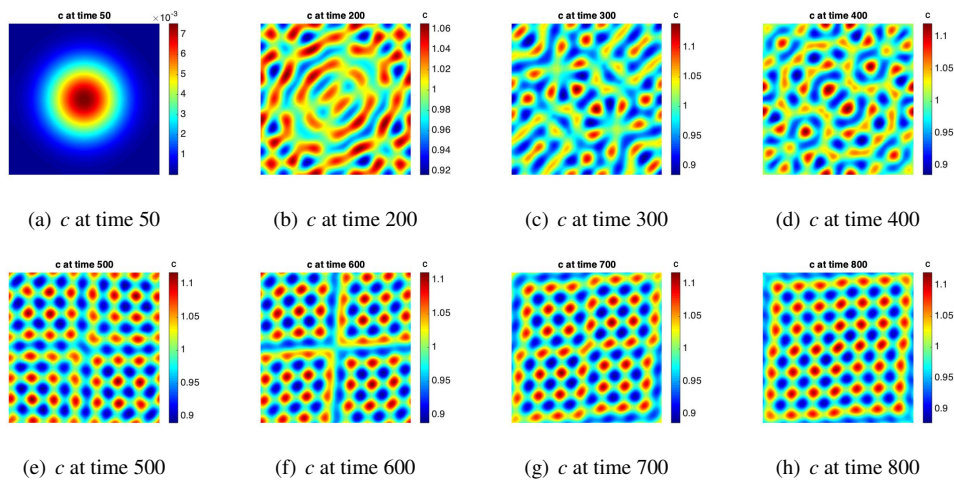


Figure 2: The dynamic process for density of self-secreted chemical with small initial distribution and  $s = -15$ ,  $g = 0.1$ .

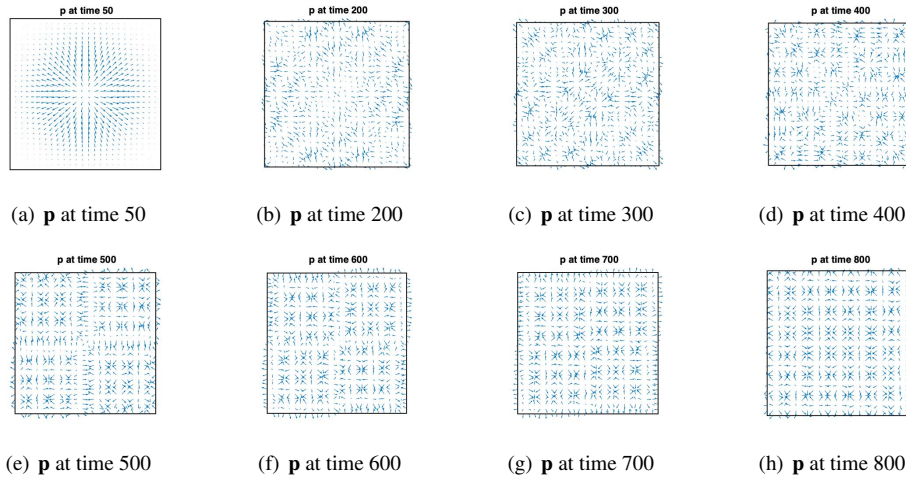


Figure 3: The dynamic process for density of polarization with small initial distribution and  $s = -15$ ,  $g = 0.1$ .

### 4.3. Chemorepulsion case 2

Here the initial condition is chosen with a small perturbation of the uniform state  $(1, 1, \mathbf{0})$ . The value of other parameters is the same as chemorepulsion case 1. The evolution of the process is presented as in Fig.4-6. We can find that clustering, pattern formation and wave appear. Comparing with case 1, the only different is the initial distribution. We could see that if the large number of bacteria live in the environment with enough self-secreted chemicals. The wave also appear just the intermediate pattern formation different. Firstly clustering appear and then it forms one line which moves along a direction with an inclination to the boundary of domain. And finally the system reaches the equilibrium state.

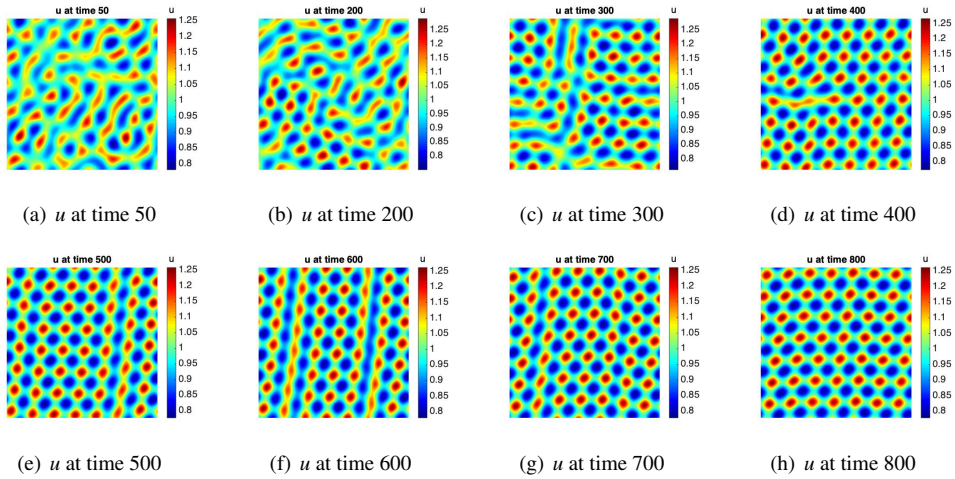


Figure 4: The dynamic process for bacterial density with large initial distribution and  $s = -15$ ,  $g = 0.1$ .

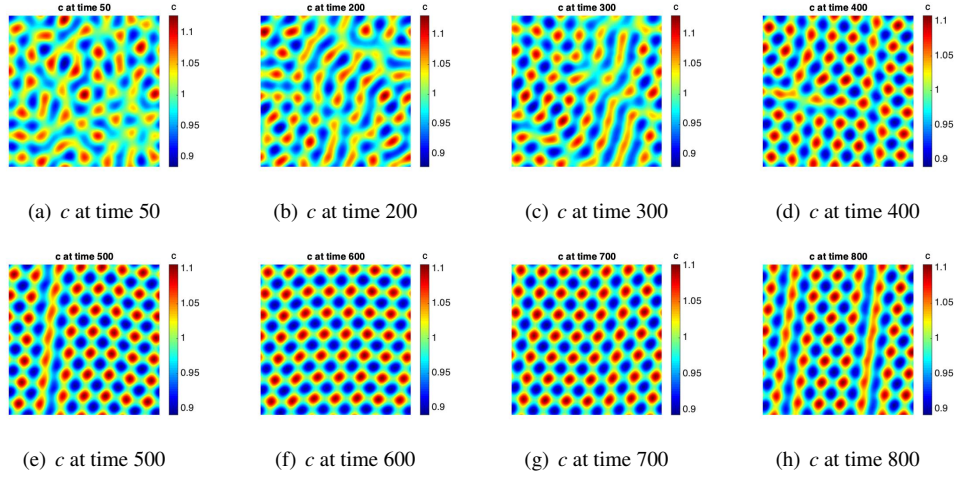


Figure 5: The dynamic process for density of self-secreted chemical with large initial distribution and  $s = -15$ ,  $g = 0.1$ .

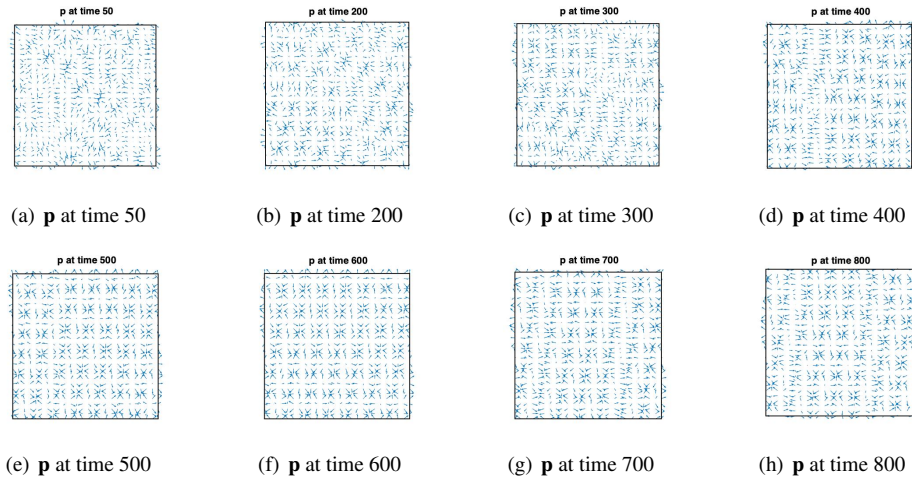


Figure 6: The dynamic process for polarization with large initial distribution and  $s = -15$ ,  $g = 0.1$ .

#### 4.4. Chemorepulsion case 3

In this subsection, the initial distribution and all the parameters are given as chemorepulsion case 1, except  $s = -25$ ,  $g = 1$ . The evolution of the process is given as in Fig.7-9. We can find that clustering and wave pattern formation appear, and finally both of them form one special order and arrive at the equilibrium state. Comparing with case 1, the value of  $g$  increases to 10 times. Which makes the diameter of clustering is smaller and the time of wave pattern formation appear early. The clustering form one line along the diagonal direction before the wave appear. And in the counter diagonal direction, part of the clustering gathering in the strip as represented in Fig.7e-h.

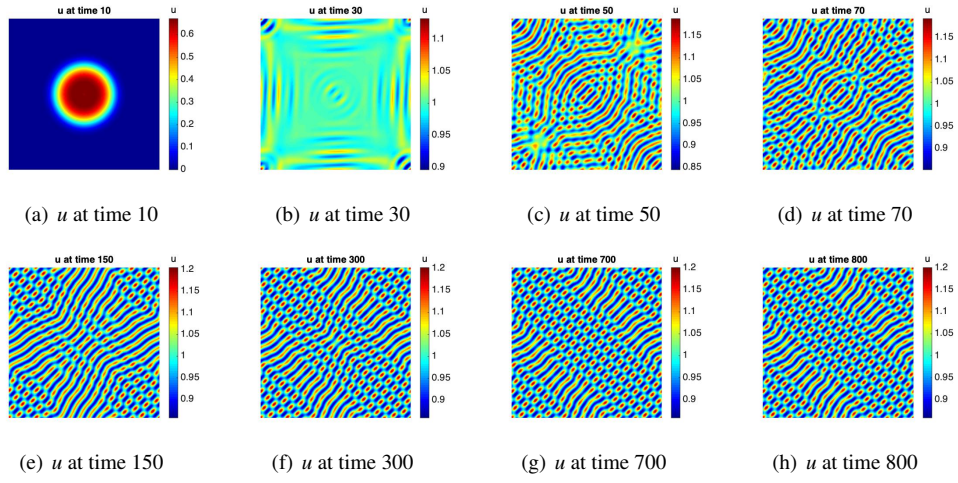


Figure 7: The dynamic process for bacterial density with small initial distribution and  $s = -25$ ,  $g = 1$ .

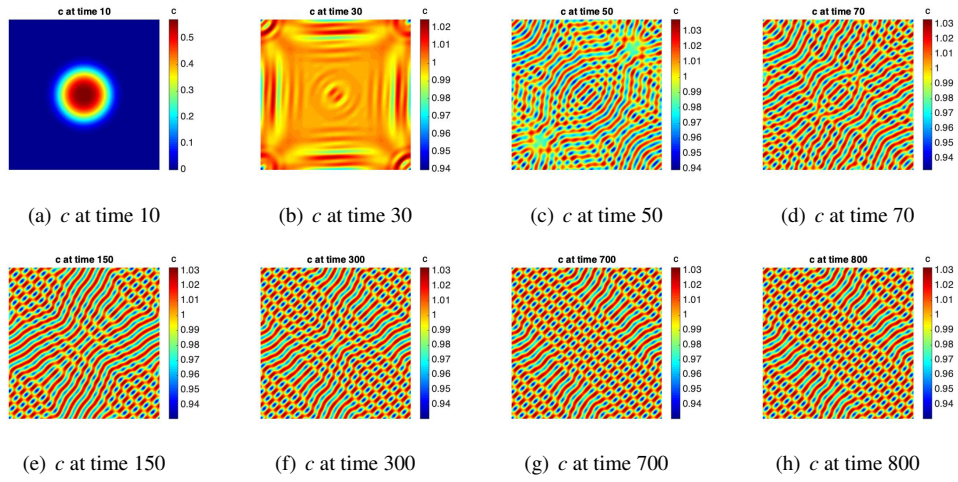


Figure 8: The dynamic process for density of self-secreted chemical with small initial distribution and  $s = -25$ ,  $g = 1$ .

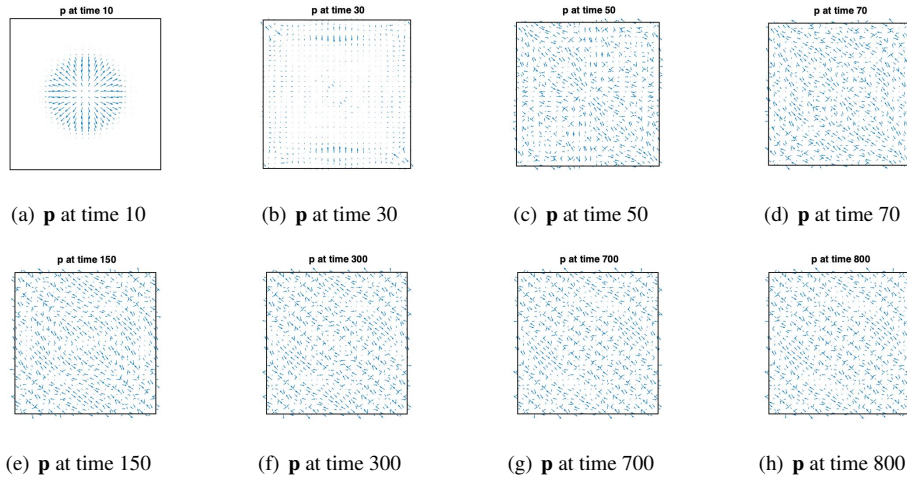


Figure 9: The dynamic process for polarization with small initial distribution and  $s = -25$ ,  $g = 1$ .

#### 4.5. Chemorepulsion case 4

For simulating the chemorepulsion case, here we choose the initial condition with a small perturbation of the uniform state  $(1, 1, \mathbf{0})$  which is the same as chemorepulsion case 2. The value of parameters is the same as chemorepulsion case 3. The evolution of the process is obtained as in Fig.10-12. We can also find that clustering and wave pattern formation appear, and finally reach the equilibrium state. Comparing with case 3, at the beginning the bacteria gather in the clustering, then quickly form the strip, and the wave pattern formation arise. In the equilibrium state, the strip pattern formation along the counter diagonal direction could break up. Which means the bacteria far away the breaking point. This is the repulsion due to the self-secreted chemical. Which confirms the theoretical analysis in the physical background as presented in [1, 6].

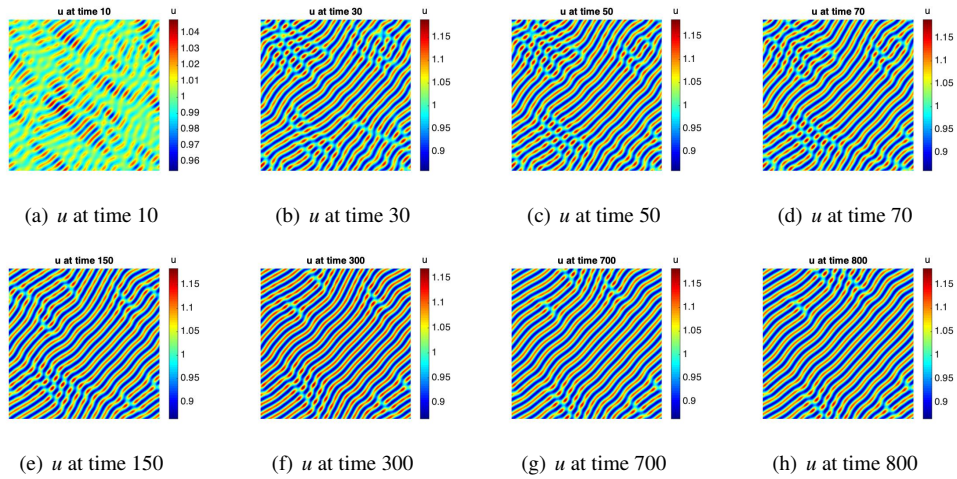


Figure 10: The dynamic process for bacterial density with large initial distribution and  $s = -25$ ,  $g = 1$ .

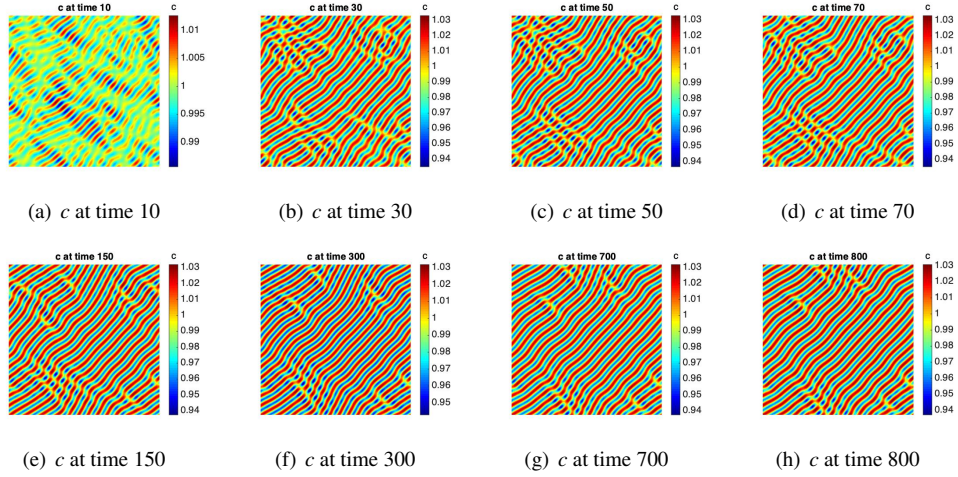


Figure 11: The dynamic process for density of self-secreted chemical with large initial distribution and  $s = -25$ ,  $g = 1$ .

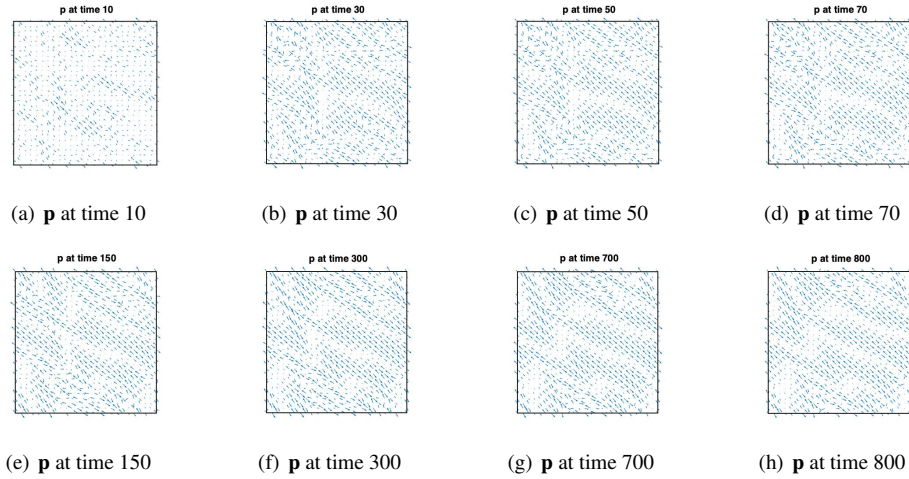


Figure 12: The dynamic process for polarization with large initial distribution and  $s = -25$ ,  $g = 1$ .

## 5. Conclusion

For simulating growth-mediated autochemotactic pattern formation in self-propelling bacteria, we propose one combined modified characteristic Galerkin finite element method. In this method, the discrete system is divided into three separated symmetric positive definite sub-problems, and keeps mass balance wholly. The convergence of the proposed method is studied and the error estimate is also derived. We present four chemorepulsion cases. Under the small value of grow rate, before the wave pattern formation arise, the clustering and strip appear. In the large value of grow rate, the bacteria gather and quickly move to the wave pattern formation and arrive at the equilibrium state. In this process, the effect of repulsion from self-secreted chemical and the initial distribution also affect the structure of the pattern before wave arising. Which confirms the theoretical analysis in the different regimes and also brings up new results for expanding the physical mechanism.



## Acknowledgments

J. Zhang's work was supported by the Fundamental Research Funds for the Central Universities (20CX05011A). M. Jiang's work was supported partially by the Natural Science Foundation of Shandong Province(Grant number ZR2021QA018). J. Zhu's work was partially supported by the National Council for Scientific and Technological Development of Brazil (CNPq). X. Yu's work was supported partially by the National Natural Science Foundation of China (Grant No. 12071046) . L. Bevilacqua's work was supported partially by CNPq/TWAS Grant, the COPPE/CAPES Grant 001, and the USP/IEA visiting research program.

## References

- [1] M. Mukherjee, Pushpita Ghosh, Growth-mediated autochemotactic pattern formation in self-propelling bacteria, *Physical Review E* 97, 012413 (2018).
- [2] J. Toner, Y. Tu, Long-Range Order in a Two-Dimensional Dynamical XY Model: How Birds Fly Together, *Phys. Rev. Lett.*, 75, 4326(1995).
- [3] E. O. Budrene, H. C. Berg, Generic modelling of cooperative growth patterns in bacterial colonies, *Nature*, 349, 630(1991).
- [4] S. Hubbard, P. Babak, S. Sigurdsson and K. Magnusson, A model of the formation of fish schools and migrations of fish, *Ecol. Modell.*, 174, 359(2004).
- [5] E. Rauch, M. Millonas and D. Chialvo, Pattern formation and functionality in swarm models, *Phys. Lett. A*, 207, 185(1995).
- [6] B. Liebchen, D. Marenduzzo, I. Pagonabarraga and M. E. Cates, Clustering and Pattern Formation in Chemorepulsive Active Colloids, *Phys. Rev. Lett.* 115, 258301(2015).
- [7] B. Liebchen, D. Marenduzzo and M. E. Cates, *Phys. Rev. Lett.* 118, 268001 (2017).
- [8] J. Zhao, X. Yang, J. Li and Q. Wang, Energy stable numerical schemes for a hydrodynamic model of nematic liquid crystals, *SIAM Journal on Scientific Computing*,38(5):3264-3290(2016).
- [9] J. Zhao, X. Yang, Y. Gong and Q. Wang, A novel linear second order unconditionally energy stable scheme for a hydrodynamic Q-tensor model of liquid crystals. *Comput. Methods Appl. Mech. Eng.* 318, 803-825 (2017).
- [10] X. Yang and D. Han Linearly first- and second-order, unconditionally energy stable schemes for the phase field crystal equation. *J. Comput. Phys.* 330, 1116-1134 (2017)
- [11] J. Shen and X. Yang, Decoupled, energy stable schemes for phase-field models of two-phase incompressible flows. *SIAM J. Numer. Anal.* 53(1), 279-296 (2015).
- [12] Y. Gong, J. Zhao and Q. Wang, Arbitrarily high-order unconditionally energy stable schemes for thermodynamically consistent gradient flow models, *SIAM J. Sci. Comput.* 42, 135-156, (2020).
- [13] Z. Guo, P. Lin, J. Lowengrub and S.M. Wise Mass conservative and energy stable finite difference methods for the quasi-incompressible Navier-Stokes-Cahn-Hilliard system: Primitive variable and projection-type schemes, *Comput. Methods. Appl. Mech. Engrg.* 326,144-174,(2017)
- [14] M. Jiang, Z. Zhang and J. Zhao, Improving the Accuracy and Consistency of the Scalar Auxiliary Variable(SAV) Method with Relaxation,*Journal of Computational Physics*,*J. Comput. Phys.*, 456, 110954(2022).

- [15] J.B. Bell, C.N. Dawson and G.R. Shubin, An unsplit high-order Godunov scheme for scalar conservation laws in two dimensions, *J. Comput. Phys.* 74, 1-24(1988).
- [16] C. Johnson, Streamline diffusion methods for problems in fluid mechanics, in: *Finite Element in Fluids VI*, Wiley, New York, 1986.
- [17] D.P. Yang, Analysis of least-squares mixed finite element methods for nonlinear nonstationary convection-diffusion problems, *Math. Comput.*, 69, 929-963(2000).
- [18] J. Douglas Jr and T.F. Russell, Numerical methods for convection-dominated diffusion problems based on combining the method of characteristics with finite element or finite difference procedures, *SIAM J. Numer. Anal.* 19, 871-885(1982).
- [19] J.S. Zhang, J. Zhu and R. Zhang, Characteristic splitting mixed finite element analysis of Keller-Segel chemotaxis models, *Appl. Math. Comput.* 278, 33-44(2016).
- [20] H. Rui and M. Tabata, A mass-conservative finite element scheme for convection-diffusion problems, *J. Sci. Comput.* 43, 416-432(2010).
- [21] M. Jiang, J. Zhang, J. Zhu, X. Yu and L. Bevilacqua, Characteristic finite element analysis of pattern formation dynamical model in polymerizing actin flocks, *App. Math. Lett.* 98, 224-232(2019).
- [22] M. Jiang, J. Zhang, J. Zhu, X. Yu and L. Bevilacqua, Numerical simulation for clustering and pattern formation in active colloids with mass-preserving characteristic finite element method, *Com. Meth. App. Mech. Eng.* 381, 113806(2021).
- [23] P.G. Ciarlet, *The finite element methods for elliptic problems*. North-Holland, New York, 1978.